Current Biology *16*, 499–505, March 7, 2006 DOI 10.1016/j.cub.2006.01.052

Report

Dorso/Ventral Genes Are Asymmetrically Expressed and Involved in Germ-Layer Demarcation during Cnidarian Gastrulation

David Q. Matus,[1] Gerald H. Thomsen,[2] and Mark Q. Martindale[1,*]
[1] Kewalo Marine Lab
Pacific Bioscience Research Center
University of Hawaii
41 Ahui Street
Honolulu, Hawaii 96813
[2] Department of Biochemistry and Cell Biology
Center for Developmental Genetics
Stony Brook University
Stony Brook, New York 11794

Summary

Cnidarians (corals, sea anemones, hydroids, and jellyfish) are a basal taxon closely related to bilaterally symmetrical animals [1–3] and have been characterized as diploblastic and as radially symmetrical around their longitudinal axis. We show that some orthologs of key bilaterian dorso/ventral (D/V) patterning genes, including the TGFβ signaling molecules *NvDpp* and *NvBMP5-8* and their antagonist *NvChordin*, are initially expressed asymmetrically at the onset of gastrulation in the anthozoan sea anemone *Nematostella vectensis*. Surprisingly, unlike flies and vertebrates, the TGFβ ligands and their antagonist are colocalized at the onset of gastrulation but then segregate by germ layer as gastrulation proceeds. TGFβ ligands, their extracellular enhancer, *NvTolloid*, and components of their downstream signaling pathway (*NvSmad1/5* and *NvSmad4*) are all coexpressed in presumptive endoderm, indicating that only planar TGFβ signaling operates at these stages. *NvChordin* expression forms a boundary between TGFβ-expressing endodermal cells and aboral ectoderm. Manipulation of nuclear β-catenin localization affects TGFβ ligand and antagonist expression, suggesting that the ancestral role of the *dpp/chordin* antagonism during gastrulation may have been in germ-layer segregation and/or epithelial patterning rather than dorsal/ventral patterning.

Results and Discussion

Cnidarians are a highly diverse group of animals that display an amazing array of life-history strategies and morphological variation in the absence of organ-level organization. Anatomically, they can be thought of as essentially epithelial animals typically described as radially organized around a primary longitudinal axis, the oral-aboral axis. Although some adult cnidarians show signs of bilaterality (e.g., the ciliated pharyngeal siphonoglyph of anthozoans) [4, 5], the homology of body-plan organization to other metazoans is poorly understood. The gut cavity (coelenteron) is lined by the endodermally derived bifunctional (absorptive and contractile) gastrodermis that in *N. vectensis* arises via unipolar invagination at the oral pole during gastrulation. The endoderm is continuous via the outer ectodermal epidermis through a single pharyngeal opening. Although there are epithelial muscle cells whose cell bodies reside in the plane of the endoderm, there is no mesodermal layer of cells separating these two epithelial layers or a centralized nervous system characteristic of bilaterally symmetrical triploblastic animals. Cnidarian genomes contain many of the genes required for mesodermal [6–9] and axial [10, 11] development in bilaterians, suggesting that these genes were co-opted into new functions in bilaterians.

Diffusible extracellular ligands of the TGFβ superfamily (e.g., *BMPs/dpp*) and their specific antagonists (*chordin/sog*) and regulators (*tolloid*) are some of the most highly conserved molecules involved in D/V patterning in both protostomes and deuterostome bilaterians [12]. Extracellular interactions between *dpp/BMP2/4* and *chordin/sog* regulate patterning of the D/V axis in animals as distantly related as flies and vertebrates [13–15]. Deuterostomes have a greater number of interacting ligands (e.g., *BMPs*, *GDFs*, and *nodals* [12, 16]), antagonists (e.g., *noggin* [12, 17], *follistatin* [18, 19], *cerberus* [20], and *gremlin* [21]), and downstream components (e.g., Smads [22, 23]), than ecdysozoan model systems [24].

Here, we explore the deployment of some of the key members of the conserved bilaterian D/V patterning pathway during gastrulation in an anthozoan cnidarian embryo to determine their potential role in animals whose ancestors diverged from the classically recognized bilaterians some 600 million years ago. We report the first expression of *chordin/sog* and tolloid orthologs outside of the Bilateria. Although initially expressed asymmetrically, it appears that the ancestral role of the *dpp/BMP2/4/chordin* antagonism during gastrulation is downstream of the nuclear β-catenin pathway and may have been involved with germ-layer segregation and/or epithelial patterning.

Coverage of the *N. vectensis* genome has been sequenced eight times by the Joint Genome Institute (Department of Energy, Walnut Creek, California), allowing for the comprehensive identification of all TGFβ family members, their antagonists, and orthologs of other components previously shown to be involved in generating the D/V axis in other systems. We have cloned six TGFβ ligands from *N. vectensis*, the sequences of five of which have recently been identified in an EST screen [25]. Of these six, only two, *NvDpp* (BMP 2/4) [11], and *NvBMP5-8*, a precursor to the vertebrate *BMP 5*, *6*, *7*, and *8* clade [26] (see Figure S1 in the Supplemental Data online), are expressed during gastrulation and will be discussed here.

Genome searches were also conducted to isolate BMP antagonists. An ortholog to the BMP antagonist *chordin/sog* (*NvChordin*) (Figure S2), which is asymmetrically expressed in the dorsal lip of the embryonic

*Correspondence: mqmartin@hawaii.edu

blastopore (e.g., *chordin* in the Spemann Organizer) and in the *Drosophila* blastoderm [12, 13], was recovered, as were orthologs to other BMP antagonists expressed in the Spemann Organizer (*NvNoggin1* and *2*, *NvFollistatin*, and *NvGremlin*). Of these Organizer genes, only *NvChordin* is expressed during gastrulation (D.Q.M., K. Pang, H. Marlow, G.H.T., and M.Q.M., unpublished data). We also recovered an important component of the TGFβ signaling system, the metalloprotease *tolloid* (*NvTolloid*), which enhances TGFβ signaling in bilaterians by cleaving *chordin* within *chordin-BMP* complexes [27]. No ortholog to *twisted gastrulation* (*tsg*), another gene that can both enhance or repress *BMP* signaling in arthropods and vertebrates [28], appears to be present in the *N. vectensis* genome. In order to determine the target of BMP signaling, we recovered orthologs to some of the downstream components of the *dpp/BMP2/4* pathway [22, 23], including two Smads (*NvSmad1/5* and *NvSmad4*). *N. vectensis* possesses four Smads (Figure S3) as well as at least six TGFβ receptors (three Type I and three Type II) (unpublished data). Thus, cnidarians have many, but not all of, the TGFβ signaling genes involved in vertebrate and fly D/V patterning [12, 13].

Anthozoan cnidarians like *N. vectensis* have been described as being bilaterally symmetrical [4, 5] as a result of the anatomy of internal mesenteries and the position of a groove of ciliated cells in the animal's pharynx (siphonoglyph). In anthozoans, this plane of symmetry runs perpendicular to the oral-aboral axis and defines the "directive axis," but the homology of the directive axis to any bilaterian axis rests on the expression of a single *N. vectensis* gene, *NvDpp* [11] (an ortholog of *dpp/BMP2/4*), which, along with its antagonist, *sog/chordin*, specifies the D/V axis of *Drosophila* and vertebrates [12, 14]. *NvDpp* is initially expressed along one edge of the blastopore during early gastrulation of *N. vectensis* [11] and the coral *Acropora* [29] and remains asymmetrically expressed as cells begin to involute during early gastrulation (Figure 1B), but its expression spreads around the blastopore, and by late gastrulation, all endodermal cells express *NvDpp* (Figure 1D). At later planula stages, *NvDpp* is expressed asymmetrically along the pharyngeal ectoderm [11].

The expression *NvBMP5-8* is nearly identical to that of *NvDpp*. Both are expressed asymmetrically on one side of the blastopore (the future oral pole) during early gastrulation (Figures 1B and 1C), and both are eventually expressed throughout the presumptive endoderm (Figures 1D and 1E). However, *NvBMP5-8* is initially expressed maternally (Figure 1A) (whereas *NvDpp* is not) before transcripts disappear and reinitiate zygotically at the onset of gastrulation (Figure 1C). *NvBMP5-8* does not show asymmetric expression in pharyngeal ectoderm during later planula stages (Figure S4). *NvDpp* and *NvBMP5-8* are members of gene families that gave rise to the vertebrate *BMP4* and *7* subclasses, respectively, and their coexpression could be functionally significant because BMP4/BMP7 heterodimers are more active than *BMP4* or *BMP7* homodimers in vertebrate assays [30, 31]. Thus, coexpression of both *NvDpp* and *NvBMP5-8* genes in presumptive endodermal tissues beginning at early gastrulation might enhance signaling activity by those cells compared to cells expressing *NvDpp* or *NvBMP5-8* alone.

NvChordin, the *N. vectensis* ortholog of the BMP inhibitor *chordin/sog* (Figure S2), is also expressed highly asymmetrically on one side of the blastopore before *NvDpp* and *NvBMP5-8* are expressed (Figure 1F). In vertebrates and flies, *chordin/sog* is expressed on the opposite side of the D/V axis from the *dpp/BMP* signal [14], but, surprisingly, this was not the case in *N. vectensis*, where double labeling shows that *NvChordin*, *NvDpp*, and *NvBMP5-8* are initially expressed on the same side of the blastopore (Figures 1G–1I and 1L). Although *NvChordin* and *NvDpp* expression remain higher on one side of the blastopore through the initial stages of gastrulation, the expression of both these genes, as well as *NvBMP5-8*, spreads to form two distinct domains (Figures 1H–1N), with *NvDpp* and *NvBMP5-8* expressed in cells at the center of the blastopore and invaginating endoderm (Figures 1K, 1L, and 1N) and *NvChordin* in cells surrounding the blastopore. As cells move internally through the blastopore, they downregulate *NvChordin* and upregulate *NvDpp* [11], *NvBMP5-8*, *NvTolloid* (Figure 1P), and a suite of genes that includes *NvExd* (Figure 1N), *NvSnail a*, *NvSnail b*, *NvFkd*, *NvGATA*, *NvTropomyosin*, *NvTwist*, and *NvMuscle lim* [6, 9]. Of particular interest at this stage is *NvTolloid*, which in metazoans proteolytically cleaves chordin, releasing BMP, and thereby potentiating BMP signaling [28]. *NvTolloid* is expressed uniformly throughout the internal endoderm in the same cells that express *NvDpp* and *NvBMP5-8* orthologs (Figure 1P).

Possible Roles of TGFβ and *NvChordin* Expression during Gastrulation

It is not yet known whether the early spatial asymmetry of *NvChordin*, *NvDpp*, and *NvBMP5-8* seen on one side of the blastopore at gastrulation corresponds to later morphological asymmetries because there are no landmarks to relate the early expression to adult anatomy, but it is interesting to speculate that their early expression reflects intrinsic embryonic properties involved in D/V patterning as in their bilaterian orthologs [12, 14, 32]. The fact that *NvChordin* is not expressed on the opposite side of the blastopore from *NvDpp* and *NvBMP5-8*, as one might predict from fly and vertebrate models [12, 14, 32], is surprising but similar to oral ectodermal expression in the animal hemisphere of sea urchin embryos [33, 34] (D. McClay, personal communication). Coincident *NvChordin* and *NvDpp* expression is similar to the transient coexpression of *BMP-2*, *BMP-4*, and *Chordin* in the zebrafish embryonic shield, but opposing TGFβ signaling and antagonism are still required for the formation of normal mesodermal and D/V patterning [35].

The coordinate expression of these genes in *N. vectensis* reflects some intrinsic developmental asymmetry in the embryo, but their main function at gastrulation stages could be to regulate something other than D/V polarity. One possibility is that TGFβ signaling could be required for endodermal cell-fate specification. The coincident expression of *NvChordin* and *NvDpp/NvBMP5-8* at the onset of gastrulation results in a latent CHORDIN/DPP/BMP5-8 protein complex in presumptive endodermal cells at the blastopore lip. Upregulation of *NvTolloid* expression by internal endodermal cells would serve to quench activity of residual *NvChordin* protein in involuting cells and release NvDPP and NvBMP5-8 ligands,

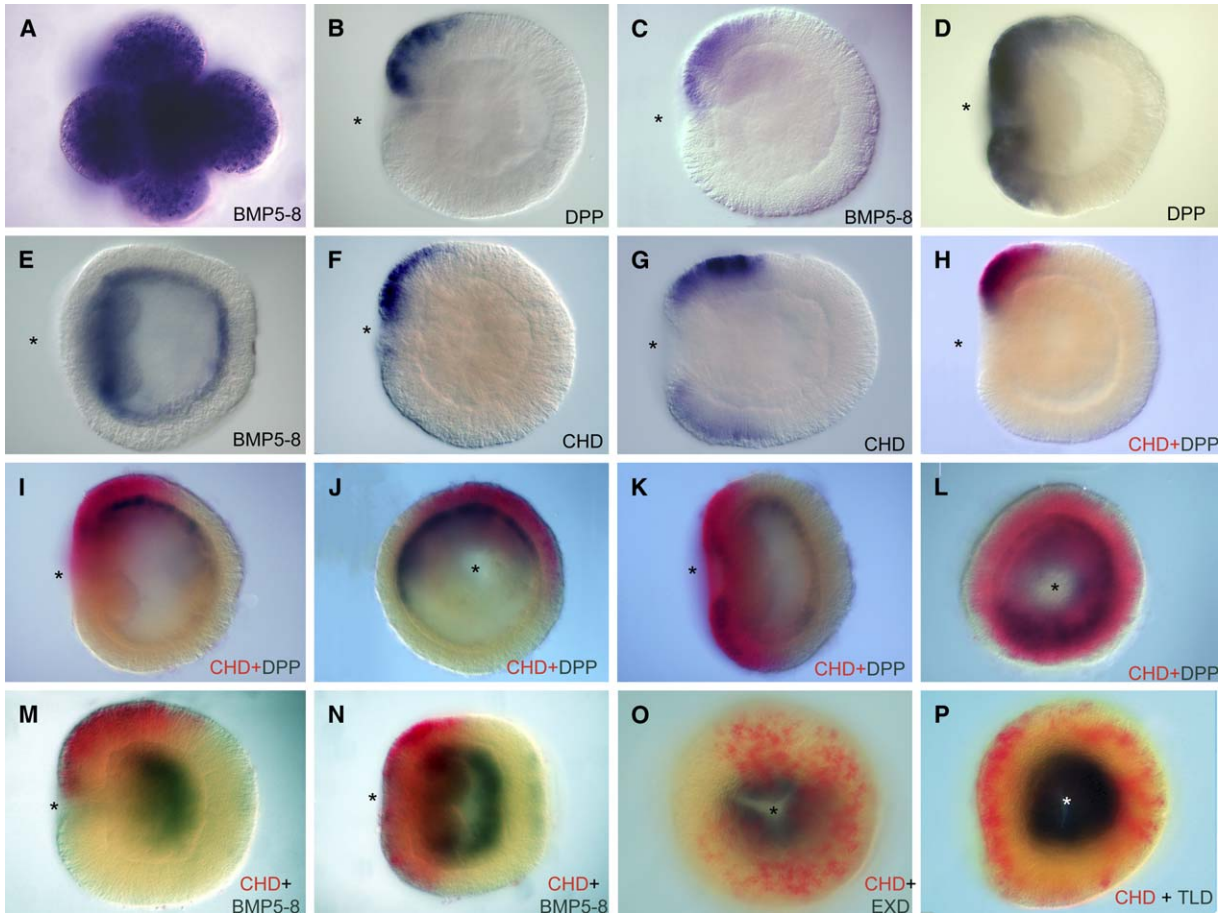

Figure 1. Asymmetric Gene Expression during *N. vectensis* Gastrulation

Whole-mount in situ hybridization of gastrulation-stage genes showing asymmetric expression.
(A) *NvBMP5-8* is initially expressed maternally in cleavage-stage embryos.
(B) *NvDpp* is initially expressed asymmetrically on one side of the blastopore.
(C) *NvBMP5-8* is also initially expressed asymmetrically during early gastrulation.
(D) By midgastrulation, *NvDpp* is expressed around the blastopore lip.
(E) At a similar developmental stage, *NvBMP5-8* is expressed in the endoderm.
(F) *NvChordin*(CHD) is also expressed asymmetrically during early gastrulation on one side of the blastopore lip.
(G) By midgastrulation, *NvChordin* is expressed around the blastopore lip in ectoderm.
(H) Double-label in situ hybridization shows that *NvChordin* (red) and *NvDpp* (blue) are expressed asymmetrically, on the same side of the blastopore during early gastrulation.
(I and J) During early–mid-gastrulation, *NvChordin* (red) remains expressed asymmetrically on one side of the blastopore in ectoderm, whereas *NvDpp* is expressed asymmetrically at the blastopore lip and in invaginating endoderm.
(K and L) Lateral and oral views of *NvDpp*/*NvChordin* mRNA expression at the end of gastrulation showing *NvChordin* (red) expressed around the blastopore in ectoderm, and *NvDpp* expressed at the blastopore lip and in endoderm.
(M) *NvBMP5-8* is expressed in the endoderm during early gastrulation, whereas *NvChordin* is expressed asymmetrically.
(N) At the end of gastrulation, *NvBMP5-8* is expressed panendodermally, whereas *NvChordin* is expressed around the blastopore in ectoderm.
(O) *NvChordin* is expressed in a punctate pattern around the blastopore lip, whereas *NvExd* (blue) is expressed in the blastopore.
(P) *NvTld* is expressed in endoderm only during gastrulation. Asterisks denote the blastopore and future mouth.
All embryos are lateral views, with anterior to the left, except (A), which is a cleavage-stage embryo, and (J), (L), (O), and (P), which are oral views.

thereby boosting BMP signaling in the endoderm. As gastrulation progresses, *NvChordin* is expressed in a ring of oral ectoderm around the external edge of the blastopore (Figures 1L and 1N), whereas the expression of *NvDpp* and *NvBMP5-8* becomes restricted to endoderm. Although the initial expression of *NvDpp* and *NvBMP5-8* in presumptive endoderm is asymmetrical (Figures 1C, 1I, and 1J), the rapid spread of *NvDpp* and *NvBMP5-8* gene expression throughout the endodermal epithelium as it invaginates during gastrulation is consistent with the fact that fly *dpp* and vertebrate *BMP4* can upregulate their own expression [36, 37] and is reminiscent of the phenomenon of planar endodermal autoinduction by TGFβ family members *nodal* and *Vg1* in vertebrates [16]. If TGFβ ligands in *N. vectensis* provide inductive signals emanating from the endodermal epithelium, one possible function for oral/blastoporal ectodermal *NvChordin* is to insulate the outer ectodermal cells from the planar spread of *BMP* signals through the blastopore.

In order to investigate whether TGFβ signaling was localized to presumptive endoderm or serves to signal overlying ectoderm, we looked at the deployment of downstream components of the *dpp*/*BMP2/4* pathway.

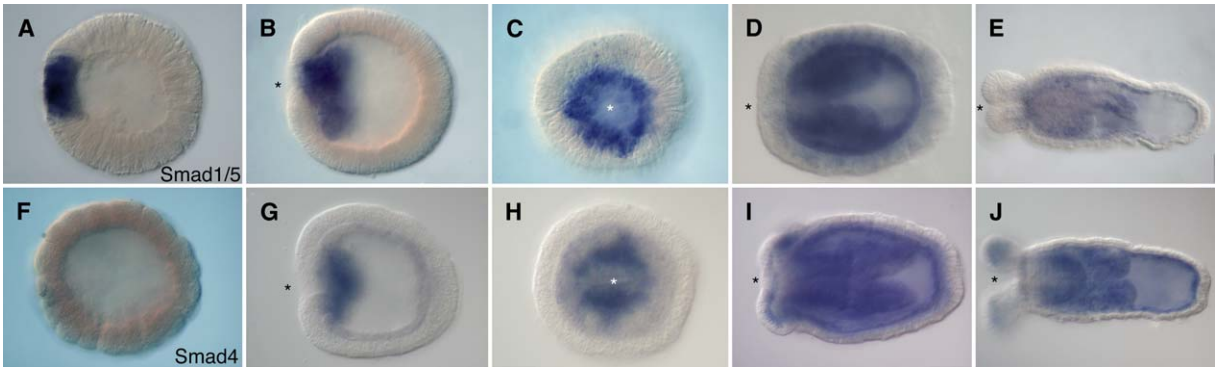

Figure 2. Expression of Downstream Components of TGFβ Signaling

NvSmad1/5 (A–E) and *NvSmad4* (F–J) are expressed in presumptive endoderm during gastrulation ([A–C] and [G and H]). *NvSmad1/5* is expressed asymmetrically in the blastula prior to the onset of gastrulation (A) and in invaginating endoderm at the blastopore during gastrulation (B and C). Expression remains in endoderm through planula (D) and polyp stages (E). *NvSmad4* is expressed in invaginating endoderm at the site of gastrulation (G and H), and remains on in endoderm though planula (I) and polyp stages (J). The asterisk denotes the blastopore and future mouth. All embryo views are lateral with anterior to the left, except (A) and (F), which are blastula views, and (C) and (H), which are oral views.

In bilaterians, binding of TGFβ ligands to their receptors (Type I and II) results in the phosphorylation of Smad proteins, which form complexes that activate transcription [23]. *NvSmad1/5* (Figure 2A) is expressed at the future site of gastrulation, and both *NvSmad1/5* and *NvSmad4* are expressed in invaginating endoderm (Figures 2B, 2C, 2G, and 2H) throughout planula and polyp stages (Figures 2D, 2E, 2I, and 2J). The fact that TGFβ ligands, *NvTolloid*, and components of their downstream signal transduction pathway (*NvSmad1/5*, *NvSmad4*) are all expressed in presumptive endoderm strongly implicates planar TGFβ signaling activity in germ-layer segregation and suggests that *NvChordin* expression likely serves to restrict the spread of TGFβ signaling to the outer ectoderm.

If TGFβ signaling is involved in endodermal cell-fate specification, it could be affected by upstream components involved in the gastrulation process. Lithium-chloride treatment of *N. vectensis* embryos prolongs the gastrulation process, resulting in an elongated planula driven by an increase in the number of cells that enter the blastopore, thus converting presumptive ectodermal cells to endoderm [38]. Lithium chloride interferes with GSK3-mediated β-catenin destruction, which in *N. vectensis* increases the number of cells around the oral pole that localize β-catenin to their nuclei (Figures 3A and 3B) [38]. We tested whether ectopically activating downstream targets of the *wnt* signaling pathway in *N. vectensis* embryos with lithium chloride affects the expression of early candidate mesendodermal patterning genes. Lithium chloride does not affect the initial asymmetry in expression of *NvChordin*, *NvDpp*, or *NvBMP5-8* (Figures 3C–3E), but it affects the boundary of TGFβ signaling and *NvChordin* expression, shifting expression toward the aboral pole (Figures 3F and 3G). *NvDpp* and *NvBMP5-8* expression expand beyond their normal endodermal pattern outside the edge of the blastopore and into cells that will eventually move through the blastopore and elongate the planula (Figures 3F, 3H, 3I, and 3K). Double-label in situ hybridization shows that the ring of *NvChordin* expression shifts farther toward the aboral pole in the ectoderm corresponding to the boundary of *NvDpp* expression (Figure 3M), and *NvChordin* remains as a ring insulating the TGFβ-expressing presumptive endoderm from aboral ectoderm (Figures 3J and 3L), effectively maintaining the ectopic ectoderm-endoderm boundary. These lithium effects are selective, however, because not all endodermally expressed genes (e.g., *NvTolloid* [Figure 3N], *NvExd* [Figure 3O], *NvSmad1/5* [Figure 3P], and *NvSmad4* [data not shown]) are initially affected by LiCl treatment. These data (Figures 4A and 4B) suggest a close functional link between early downstream components of the canonical *wnt* signaling pathway (*NvDpp*, *NvBMP5-8*, and *NvChordin*) and initial germ-layer delineation, but not the initial asymmetric expression of *NvDpp*, *NvBMP5-8*, and *NvChordin* that must be controlled by a distinct mechanism. It is of some interest that Smad expression in *N. vectensis* occurs at the site of gastrulation; these components have been shown to integrate both TGFβ and *wnt* signaling pathways (through the formation of Smad-TCF complexes) in both frog [39] and mouse [40]. It appears that the interaction of these major signal transduction pathways during development is an ancient one, predating the cnidarian–bilaterian divergence.

The endoderm of *N. vectensis* appears to express many of the same genes involved in endoderm/endomesoderm patterning in other bilaterians [9, 41–43], and the site of gastrulation (and the site of endomesoderm formation) in both deuterostomes and cnidarians is determined by the position of cells that acquire the nuclear localization of β-catenin. The position of this nuclear localization relative to the primary egg axis is radically different between these two metazoan forms, however, occurring at the animal pole in *N. vectensis* [38], the vegetal pole in urchins [44], and the dorsal lip of the blastopore in vertebrates [45, 46]. In sea urchins, vertebrates, and cnidarians, *BMP*s are expressed in the animal hemisphere, but this region gives rise to ectodermal fates in urchins [47] and vertebrates [44–46], whereas in *N. vectensis*, this region gives rise to endodermal fates. Thus, although we propose a role for BMPs and their antagonists in germ-layer formation in *N. vectensis*, they do not appear to be strictly related to specific cell types/germ layers, but retain their expression pattern relative to

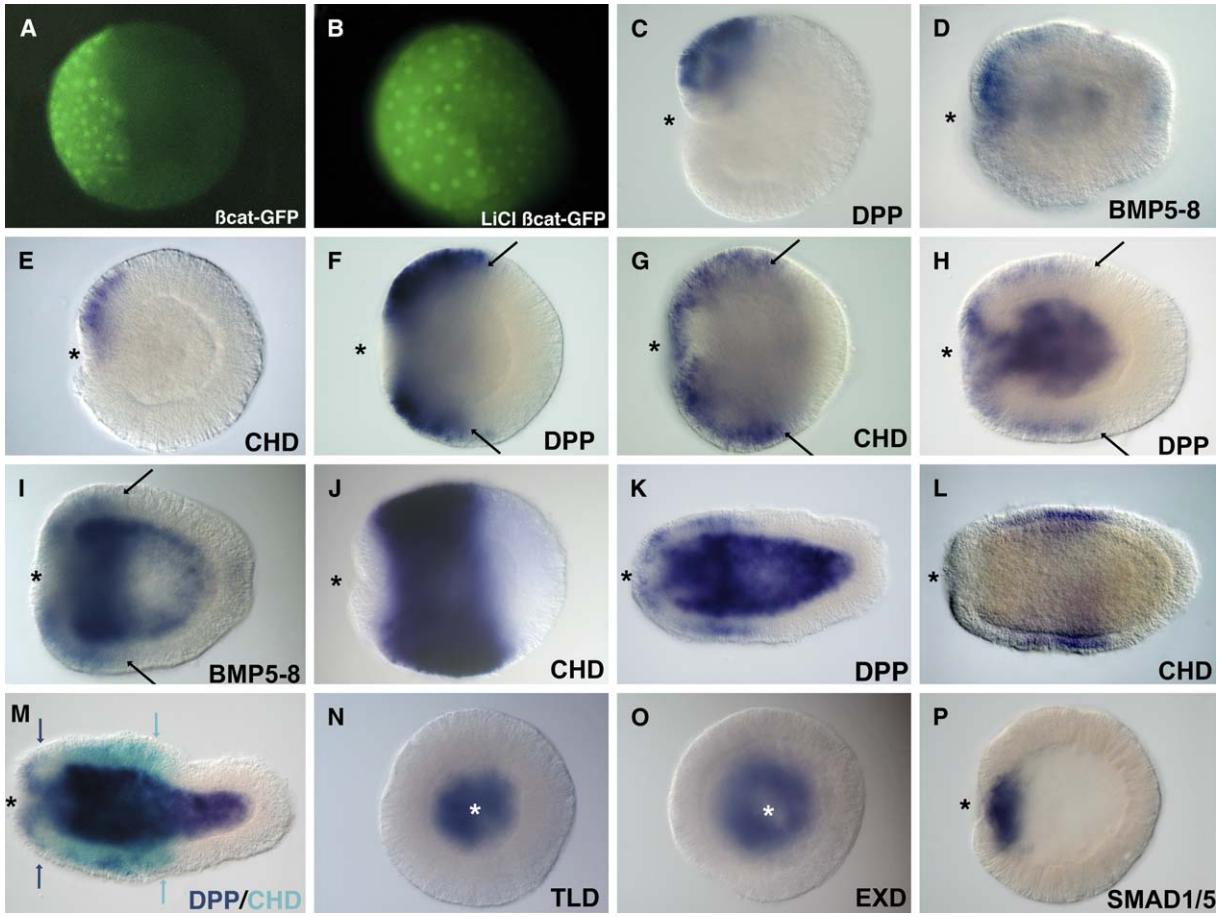

Figure 3. Lithium-Chloride Treatment Affects Gene Expression during Development

(A–E) Lithium-chloride treatment results in an increase in nuclear β-catenin (A–B). *NvDpp* (C), *NvBMP5-8* (D), and *NvChordin* (E) retain their asymmetrical expression pattern during early gastrulation.

(F and G) LiCl treatment both upregulates and shifts the expression boundary toward the aboral pole (arrows show boundary) during midgastrulation, for the *NvDPP* (F) and *NvChordin* (G).

(H and I) Both *NvDpp* (H) and *NvBMP5-8* (I) continue to be expressed in oral ectoderm during planula stages.

(J) *NvCHD* is expressed in an ectodermal band during planula stages.

(K and L) LiCl treatment results in a failure to metamorphose into polyps. *NvDpp* (K) is expressed in oral ectoderm instead of just endoderm, as it would be in untreated embryos.

(L) *NvCHD* is expressed in an ectodermal band midway along the oral-aboral axis in LiCl-treated polyp-age (72 hr) embryos.

(M) Double-label in situ hybridization of a LiCl-treated planula showing expression of *NvDpp* (blue) in oral ectoderm as well as endoderm, and *NvCHD* (light blue) in ectoderm shifted toward the aboral pole.

(N–P) LiCl treatment does not perturb the expression of *NvTld* (N), *NvExd* (O), and *NvSmad1/5* (P) during gastrulation and at planula/polyp stages (data not shown). Asterisks denote blastopore or mouth. All embryo views are lateral, with anterior to the left, except (N) and (O), which are oral views.

the primary egg axis. This is in contrast to genes that are expressed at the site of gastrulation at the animal pole in *N. vectensis*, such as *wnt* [48] and *brachyury* [42], which have moved in association with the site of gastrulation to more vegetal locations in deuterostomes such as urchins and vertebrates. Changes in the molecular control of gastrulation and cell-type specification would appear to be important components of metazoan body-plan evolution.

Conclusions

Although the molecular components of TGFβ signaling at gastrulation appear conserved between *N. vectensis* and bilaterians (*dpp/chordin/tolloid*), their deployment has been radically changed, with the ligand and antagonist both expressed asymmetrically on the same side of the blastopore in cnidarians. The relationship between this initial asymmetry and any morphological asymmetry is currently unknown. However, the later segregation of expression of the antagonist (*NvChordin*) to oral ectoderm, and ligands (*NvDpp/NvBMP5-8*), enhancers (*NvTolloid*), and downstream components (*NvSmad1/5* and *NvSmad4*) to endoderm, suggests that the ancestral function of this signaling system may have been in establishing germ-layer identity and/or a boundary for epithelial patterning rather than patterning a dorsal/ventral axis.

Experimental Procedures

Isolation of Genes from *N. vectensis*

TblastN searches of the NCBI trace archive of the *Nematostella vectensis* genome were performed with metazoan orthologs of

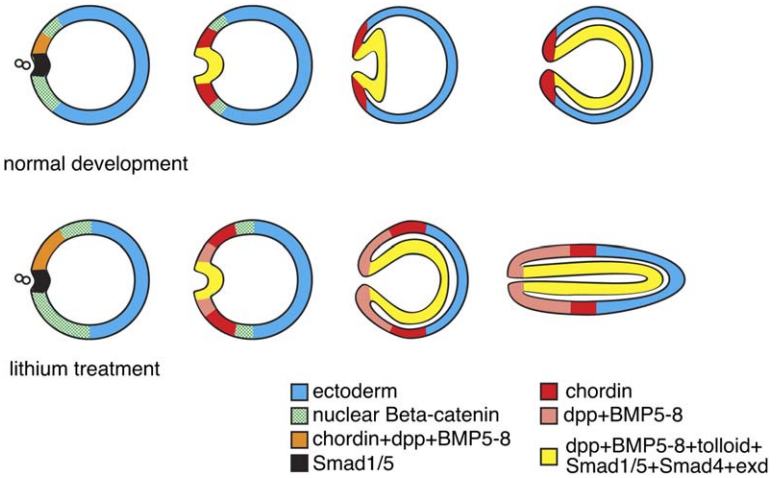

Figure 4. Summary of the Expression of TGFβ Ligands, Antagonist, and Downstream Components during Normal and Lithium-Chloride-Treated Development in *N. vectensis*

Expression of bilaterian patterning genes during gastrulation in normal (A) and lithium-treated (B) *N. vectensis* embryos. The anterior pole (animal) is the site of gastrulation and is marked by the polar bodies (small circles) to the left. Lithium-chloride treatment shifts the expression boundary for the TGFβ ligands (*NvDPP* and *NvBMP5-8*) and their antagonist (*NvChordin*) toward the aboral pole. Downstream components of classical TGFβ signaling (*NvTld*, *NvSmad1/5*, and *NvSmad4*) as well as general endodermal markers (*NvExd*) appear unaffected by lithium-chloride treatment.

bilaterian D/V patterning genes. The traces were then compiled into contigs by using AssemblyLign (Acelyris) and Sequencher (GeneCodes), and open reading frames were determined on the basis of BlastX searches against the nr database at NCBI. Gene-specific primers were then designed for 5′ and 3′ RACE with annealing temperatures between 68°C and 70°C. RACE was performed with the Smart Race cDNA amplification kit (BD Biosciences Clontech). RACE products were cloned in a plasmid vector (P-Gem T easy, Promega) and sequenced at GeneGateway (CA). Overlapping 5′ and 3′ RACE fragments were aligned and submitted to GenBank as composite transcripts DQ358699–DQ358704 (see Accession Numbers). Gene-specific primer sequences are available upon request.

Phylogenetic Analyses

Phylogenetic analysis of the TGFβ family, chordin/sog, and Smad genes were performed in order to determine orthology. *N. vectensis* genes were analyzed via BlastX searches of the GenBank database (http://www.ncbi.nlm.nih.gov/BLAST/). Amino acid alignments were made with MacVector (CLUSTALW) and corrected by hand for obvious alignment errors. MrBayes [49] was used to conduct a Bayesian phylogenetic analysis, with the "wag" amino acid model option and 1,000,000 generations sampled every 100 generations and four chains. A "consensus tree" was produced with PAUP*4.0b10 [50] from the last 9,500 trees representing 950,000 stationary generations. Posterior probabilities were calculated from this "consensus." Additionally, neighbor joining (using mean amino acid distances) and parsimony analyses were conducted with PAUP* version 4.0b10 with 1,000 bootstrap replicates. Nexus alignment files and accession numbers are available upon request.

In Situ Hybridization

In situ hybridizations with 1–3 kb digoxygenin and fluorscein-labeled antisense ribonucleotide probes were performed to follow transcript distribution as previously described [9], although a less stringent SSC concentration was used in double-label experiments (0.2× versus 0.05× in single-label experiments). Probe concentrations ranged from 1.0–2.0 ng/μl, and hybridizations were performed at 60°C for 24–48 hr. Alkaline phosphatase reaction products were visualized with NBT-BCIP (for blue dig-labeled probes), BCIP only (for light-blue dig-labeled probes), and FastRed (Sigma; for fluorescein-labeled probes). Specimens were photographed on a Zeiss Axioplan and AxioImager with a Nikon Coolpix 990 digital camera. Detailed protocols are available upon request (mqmartin@hawaii.edu).

Lithium-Chloride Experiments

Fertilized *N. vectensis* embryos were dejellied in a 2% cysteine solution in 1/3× filtered sea water for 10 min and then rinsed three times in filtered sea water. Dejellied embryos were then cultured in a 25 mM solution of LiCl in 1/3× filtered sea water and fixed for in situ hybridization [9] at different time points during development. In situ hybridizations with digoxygenin and fluorscein-labeled antisense ribonucleotide probes were performed on LiCl-treated embryos as detailed above.

Supplemental Data

Supplemental Data include four figures and are available with this article online at: http://www.current-biology.com/cgi/content/full/16/5/499/DC1/.

Acknowledgments

G.H.T. thanks W. Lennarz for sabbatical leave and members of the M.Q.M. and Kewalo Marine Lab for their generosity during his sabbatical. We thank Julia Todorov for assistance with anemones and embryos. This work was supported by grants from the NSF and NASA to M.Q.M. and NIH Grant HD032429 to G.H.T.

Received: October 31, 2005
Revised: January 11, 2006
Accepted: January 19, 2006
Published: March 6, 2006

References

1. Collins, A.G. (2002). Phylogeny of Medusozoa and the evolution of cnidarian life cycles. J. Evol. Biol. *15*, 418–432.
2. Medina, M., Collins, A.G., Silberman, J.D., and Sogin, M.L. (2001). Evaluating hypotheses of basal animal phylogeny using complete sequences of large and small subunit rRNA. Proc. Natl. Acad. Sci. USA *98*, 9707–9712.
3. Wainright, P.O., Hinkle, G., Sogin, M.L., and Stickel, S.K. (1993). Monophyletic origins of the metazoa: An evolutionary link with fungi. Science *260*, 340–342.
4. Delage, Y., and Herouard, E. (1901). Traité de Zoologie Concrète, Les Coelenterates, *Volume 2* (Paris: Libraire C. Reinwald).
5. Hyman, L.H. (1940). The Invertebrates: Protozoa through Ctenophora (New York: McGraw-Hill).
6. Fritzenwanker, J.H., Saina, M., and Technau, U. (2004). Analysis of forkhead and snail expression reveals epithelial-mesenchymal transitions during embryonic and larval development of Nematostella vectensis. Dev. Biol. *275*, 389–402.
7. Scholz, C.B., and Technau, U. (2003). The ancestral role of Brachyury: Expression of NemBra1 in the basal cnidarian Nematostella vectensis (Anthozoa). Dev. Genes Evol. *212*, 563–570.
8. Spring, J., Yanze, N., Josch, C., Middel, A.M., Winninger, B., and Schmid, V. (2002). Conservation of Brachyury, Mef2, and Snail in the myogenic lineage of jellyfish: A connection to the mesoderm of bilateria. Dev. Biol. *244*, 372–384.
9. Martindale, M.Q., Pang, K., and Finnerty, J.R. (2004). Investigating the origins of triploblasty: 'Mesodermal' gene expression in a diploblastic animal, the sea anemone Nematostella vectensis (phylum, Cnidaria; class, Anthozoa). Development *131*, 2463–2474.

10. Galliot, B. (2000). Conserved and divergent genes in apex and axis development of cnidarians. Curr. Opin. Genet. Dev. *10*, 629–637.
11. Finnerty, J.R., Pang, K., Burton, P., Paulson, D., and Martindale, M.Q. (2004). Origins of bilateral symmetry: Hox and dpp expression in a sea anemone. Science *304*, 1335–1337.
12. De Robertis, E.M., and Kuroda, H. (2004). Dorsal-ventral patterning and neural induction in Xenopus embryos. Annu. Rev. Cell Dev. Biol. *20*, 285–308.
13. Holley, S.A., and Ferguson, E.L. (1997). Fish are like flies are like frogs: Conservation of dorsal-ventral patterning mechanisms. Bioessays *19*, 281–284.
14. De Robertis, E.M., and Sasai, Y. (1996). A common plan for dorsoventral patterning in Bilateria. Nature *380*, 37–40.
15. Dale, L., and Wardle, F.C. (1999). A gradient of BMP activity specifies dorsal-ventral fates in early Xenopus embryos. Semin. Cell Dev. Biol. *10*, 319–326.
16. Schier, A.F. (2003). Nodal signaling in vertebrate development. Annu. Rev. Cell Dev. Biol. *19*, 589–621.
17. Streit, A., and Stern, C.D. (1999). Neural induction. A bird's eye view. Trends Genet. *15*, 20–24.
18. Hemmati-Brivanlou, A., Kelly, O.G., and Melton, D.A. (1994). Follistatin, an antagonist of activin, is expressed in the Spemann organizer and displays direct neuralizing activity. Cell *77*, 283–295.
19. Khokha, M.K., Yeh, J., Grammer, T.C., and Harland, R.M. (2005). Depletion of three BMP antagonists from Spemann's organizer leads to a catastrophic loss of dorsal structures. Dev. Cell *8*, 401–411.
20. Kuroda, H., Wessely, O., and De Robertis, E.M. (2004). Neural induction in Xenopus: Requirement for ectodermal and endomesodermal signals via Chordin, Noggin, beta-Catenin, and Cerberus. PLoS Biol. *2*, E92.
21. Hsu, D.R., Economides, A.N., Wang, X., Eimon, P.M., and Harland, R.M. (1998). The Xenopus dorsalizing factor Gremlin identifies a novel family of secreted proteins that antagonize BMP activities. Mol. Cell *1*, 673–683.
22. Nakayama, T., Cui, Y., and Christian, J.L. (2000). Regulation of BMP/Dpp signaling during embryonic development. Cell. Mol. Life Sci. *57*, 943–956.
23. Massague, J., Seoane, J., and Wotton, D. (2005). Smad transcription factors. Genes Dev. *19*, 2783–2810.
24. Mineta, K., Nakazawa, M., Cebria, F., Ikeo, K., Agata, K., and Gojobori, T. (2003). Origin and evolutionary process of the CNS elucidated by comparative genomics analysis of planarian ESTs. Proc. Natl. Acad. Sci. USA *100*, 7666–7671.
25. Technau, U., Rudd, S., Maxwell, P., Gordon, P.M., Saina, M., Grasso, L.C., Hayward, D.C., Sensen, C.W., Saint, R., Holstein, T.W., et al. (2005). Maintenance of ancestral complexity and non-metazoan genes in two basal cnidarians. Trends Genet. *21*, 633–639.
26. Reinhardt, B., Broun, M., Blitz, I.L., and Bode, H.R. (2004). HyBMP5–8b, a BMP5–8 orthologue, acts during axial patterning and tentacle formation in hydra. Dev. Biol. *267*, 43–59.
27. Yamamoto, Y., and Oelgeschlager, M. (2004). Regulation of bone morphogenetic proteins in early embryonic development. Naturwissenschaften *91*, 519–534.
28. Oelgeschlager, M., Larrain, J., Geissert, D., and De Robertis, E.M. (2000). The evolutionarily conserved BMP-binding protein Twisted gastrulation promotes BMP signalling. Nature *405*, 757–763.
29. Hayward, D.C., Samuel, G., Pontynen, P.C., Catmull, J., Saint, R., Miller, D.J., and Ball, E.E. (2002). Localized expression of a dpp/BMP2/4 ortholog in a coral embryo. Proc. Natl. Acad. Sci. USA *99*, 8106–8111.
30. Eimon, P.M., and Harland, R.M. (1999). In Xenopus embryos, BMP heterodimers are not required for mesoderm induction, but BMP activity is necessary for dorsal/ventral patterning. Dev. Biol. *216*, 29–40.
31. Nishimatsu, S., and Thomsen, G.H. (1998). Ventral mesoderm induction and patterning by bone morphogenetic protein heterodimers in Xenopus embryos. Mech. Dev. *74*, 75–88.
32. Araujo, H., and Bier, E. (2000). sog and dpp exert opposing maternal functions to modify toll signaling and pattern the dorsoventral axis of the Drosophila embryo. Development *127*, 3631–3644.
33. Duboc, V., Rottinger, E., Besnardeau, L., and Lepage, T. (2004). Nodal and BMP2/4 signaling organizes the oral-aboral axis of the sea urchin embryo. Dev. Cell *6*, 397–410.
34. Bradham, C.A., and McClay, D.R. (2006). p38 MAPK is essential for secondary axis specification and patterning in sea urchin embryos. Development *133*, 21–32.
35. Kishimoto, Y., Lee, K.H., Zon, L., Hammerschmidt, M., and Schulte-Merker, S. (1997). The molecular nature of zebrafish swirl: BMP2 function is essential during early dorsoventral patterning. Development *124*, 4457–4466.
36. Juan, H., and Hamada, H. (2001). Roles of nodal-lefty regulatory loops in embryonic patterning of vertebrates. Genes Cells *6*, 923–930.
37. Reversade, B., Kuroda, H., Lee, H., Mays, A., and De Robertis, E.M. (2005). Depletion of Bmp2, Bmp4, Bmp7 and Spemann organizer signals induces massive brain formation in Xenopus embryos. Development *132*, 3381–3392.
38. Wikramanayake, A.H., Hong, M., Lee, P.N., Pang, K., Byrum, C.A., Bince, J.M., Xu, R., and Martindale, M.Q. (2003). An ancient role for nuclear beta-catenin in the evolution of axial polarity and germ layer segregation. Nature *426*, 446–450.
39. Nishita, M., Hashimoto, M.K., Ogata, S., Laurent, M.N., Ueno, N., Shibuya, H., and Cho, K.W. (2000). Interaction between Wnt and TGF-beta signalling pathways during formation of Spemann's organizer. Nature *403*, 781–785.
40. Theil, T., Aydin, S., Koch, S., Grotewold, L., and Ruther, U. (2002). Wnt and Bmp signalling cooperatively regulate graded Emx2 expression in the dorsal telencephalon. Development *129*, 3045–3054.
41. Hayward, D.C., Miller, D.J., and Ball, E.E. (2004). snail expression during embryonic development of the coral Acropora: Blurring the diploblast/triploblast divide? Dev. Genes Evol. *214*, 257–260.
42. Technau, U., and Scholz, C.B. (2003). Origin and evolution of endoderm and mesoderm. Int. J. Dev. Biol. *47*, 531–539.
43. Technau, U. (2001). Brachyury, the blastopore and the evolution of the mesoderm. Bioessays *23*, 788–794.
44. Logan, C.Y., Miller, J.R., Ferkowicz, M.J., and McClay, D.R. (1999). Nuclear beta-catenin is required to specify vegetal cell fates in the sea urchin embryo. Development *126*, 345–357.
45. Larabell, C.A., Torres, M., Rowning, B.A., Yost, C., Miller, J.R., Wu, M., Kimelman, D., and Moon, R.T. (1997). Establishment of the dorso-ventral axis in Xenopus embryos is presaged by early asymmetries in beta-catenin that are modulated by the Wnt signaling pathway. J. Cell Biol. *136*, 1123–1136.
46. Schneider, S., Steinbeisser, H., Warga, R.M., and Hausen, P. (1996). Beta-catenin translocation into nuclei demarcates the dorsalizing centers in frog and fish embryos. Mech. Dev. *57*, 191–198.
47. Davidson, E.H., Cameron, R.A., and Ransick, A. (1998). Specification of cell fate in the sea urchin embryo: Summary and some proposed mechanisms. Development *125*, 3269–3290.
48. Kusserow, A., Pang, K., Sturm, C., Hrouda, M., Lentfer, J., Schmidt, H.A., Technau, U., von Haeseler, A., Hobmayer, B., Martindale, M.Q., et al. (2005). Unexpected complexity of the Wnt gene family in a sea anemone. Nature *433*, 156–160.
49. Huelsenbeck, J.P., and Ronquist, F. (2001). MRBAYES: Bayesian inference of phylogenetic trees. Bioinformatics *17*, 754–755.
50. Swofford, D.L. (2002). PAUP*: Phylogenetic Analysis Using Parsimony (*and Other Methods) Version 4 (Sunderland, MA: Sinauer Associates).

Accession Numbers

The GenBank accession number for the six genes reported in this paper are as follows: NvBMP5-8, DQ358699; NvChordin, DQ358700; NvSmad1/5, DQ358701; NvSmad4, DQ358702; NvExd, DQ358703; and NvTolloid, DQ358704.

Supplemental Data

Dorso/Ventral Genes Are Asymmetrically Expressed and Involved in Germ-Layer Demarcation during Cnidarian Gastrulation

David Q. Matus, Gerald H. Thomsen, and Mark Q. Martindale

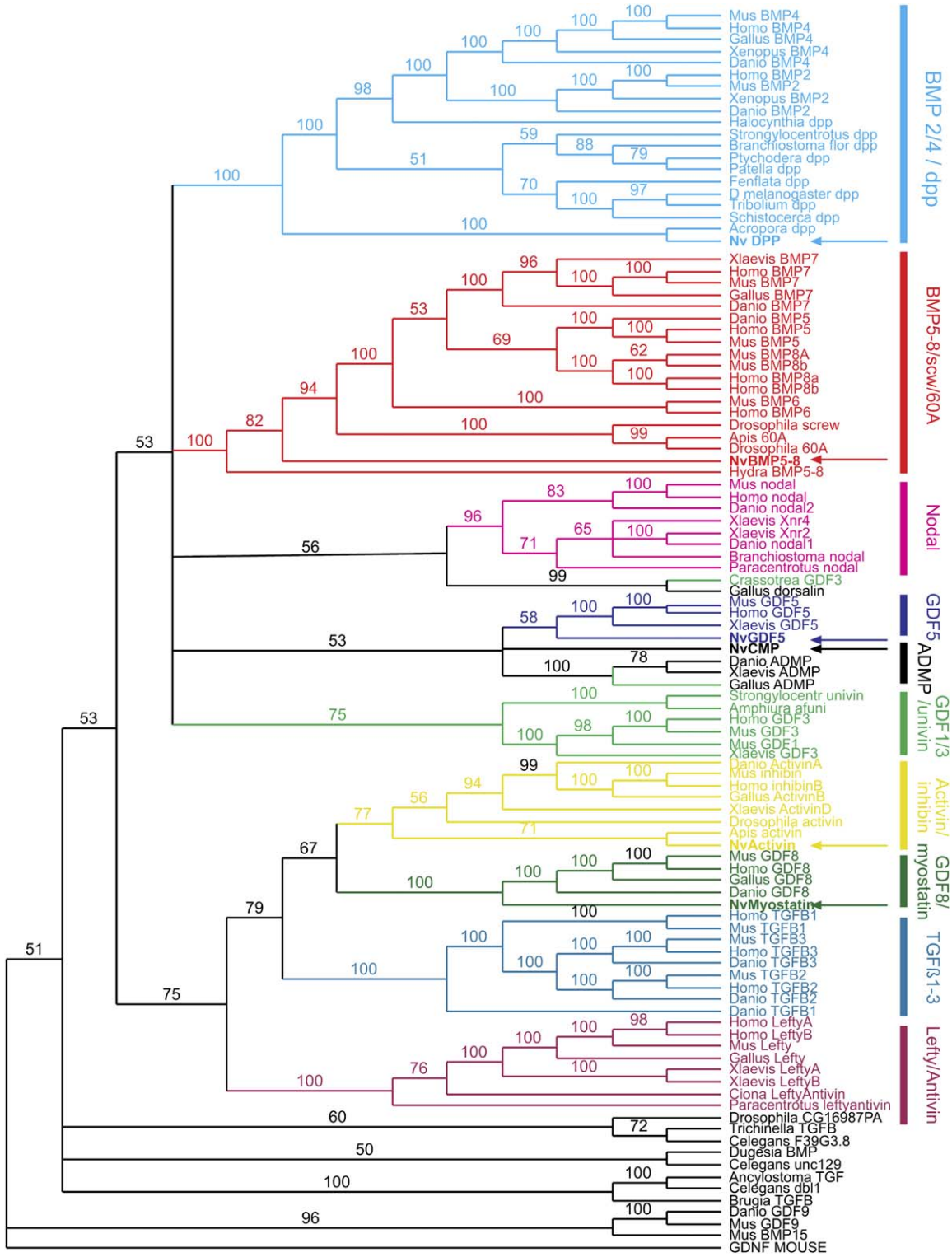

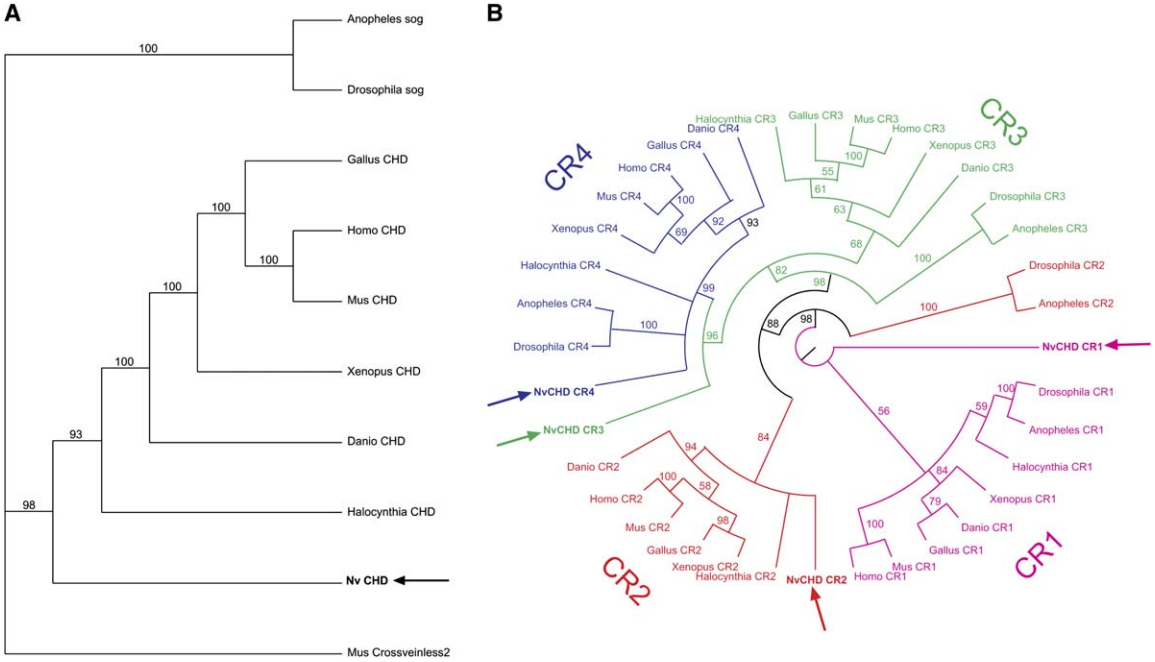

Figure S2. Bayesian Phylogenetic Analysis of Metazoan *chordin/sog* Genes

(A) A Bayesian phylogenetic analysis was conducted with near-full-length amino acid sequences of metazoan chordin/sog orthologs, with the "wag" amino acid model option in MrBayes [S1] and 1,000,000 generations sampled every 100 generations and four chains. A consensus tree was produced with PAUP*4.0b10 [S2] from the last 9,500 trees representing 950,000 stationary generations. Numbers above branches represent posterior probabilities, calculated from this consensus. The *N. vectensis chordin* sequence clusters as a sister group to deuterostome (ascidian and vertebrate) chordin genes, whereas the arthropod *sog* genes cluster together.

(B) Bayesian consensus tree of the cysteine-rich (CR) domains found in the cysteine knot gene family that includes metazoan *chordin/sog* genes. *Chordin/sog* genes contain four CR domains, which are believed to have arisen from an ancestral *chordin/sog* gene that possessed four CR domains [S4]. The *N. vectensis chordin* gene (*NvChordin*) possesses four CR domains, of which three CR domains (Nv CR1, 2, and 4) show a sister-group relationship to their metazoan CR-domain representatives. These phylogenetic analyses argue that *N. vectensis* possesses a definitive *chordin/sog* ortholog.

Figure S1. Bayesian Consensus Tree of the Metazoan TGFβ Family

Through a combination of degenerate PCR and in silico searches of the NCBI trace archive of the *N. vectensis* genome, six TGFβ genes were isolated. These traces were compiled into genomic contigs, and the contigs were analyzed via BlastX searches of the GenBank database (http://www.ncbi.nlm.nih.gov/BLAST/). A Bayesian phylogenetic analysis was conducted with the "wag" amino acid model option in MrBayes [S1] and 1,000,000 generations sampled every 100 generations and four chains. A consensus tree was produced with PAUP*4.0b10 [S2] from the last 9,500 trees representing 950,000 stationary generations. Numbers above branches represent posterior probabilities, calculated from this consensus. The phylogeny reported here agrees largely with that of Technau et al. [S3], although we recovered an additional TGFβ ligand, *NvCMP*, that they failed to isolate. Additionally, the taxon sampling used in this analysis (105 TGFβ ligands) is more thorough than that of Technau et al. [S3] (41 TGFβ ligands). The Bayesian analysis shows that *N. vectensis* possesses definitive orthologs to several TGFβ ligand subfamilies, including *dpp/BMP2/4*, *BMP5-8*, vertebrate *activin*, vertebrate *myostatin*, and *GDF-5*. A sixth TGFβ gene found in the *N. vectensis* genome may be related to both vertebrate *GDF5* and *ADMP* genes. It appears that *N. vectensis* lacks an ortholog to either the *nodal* or *lefty* families of TGFβ ligands. Nexus alignment files and accession numbers are available upon request.

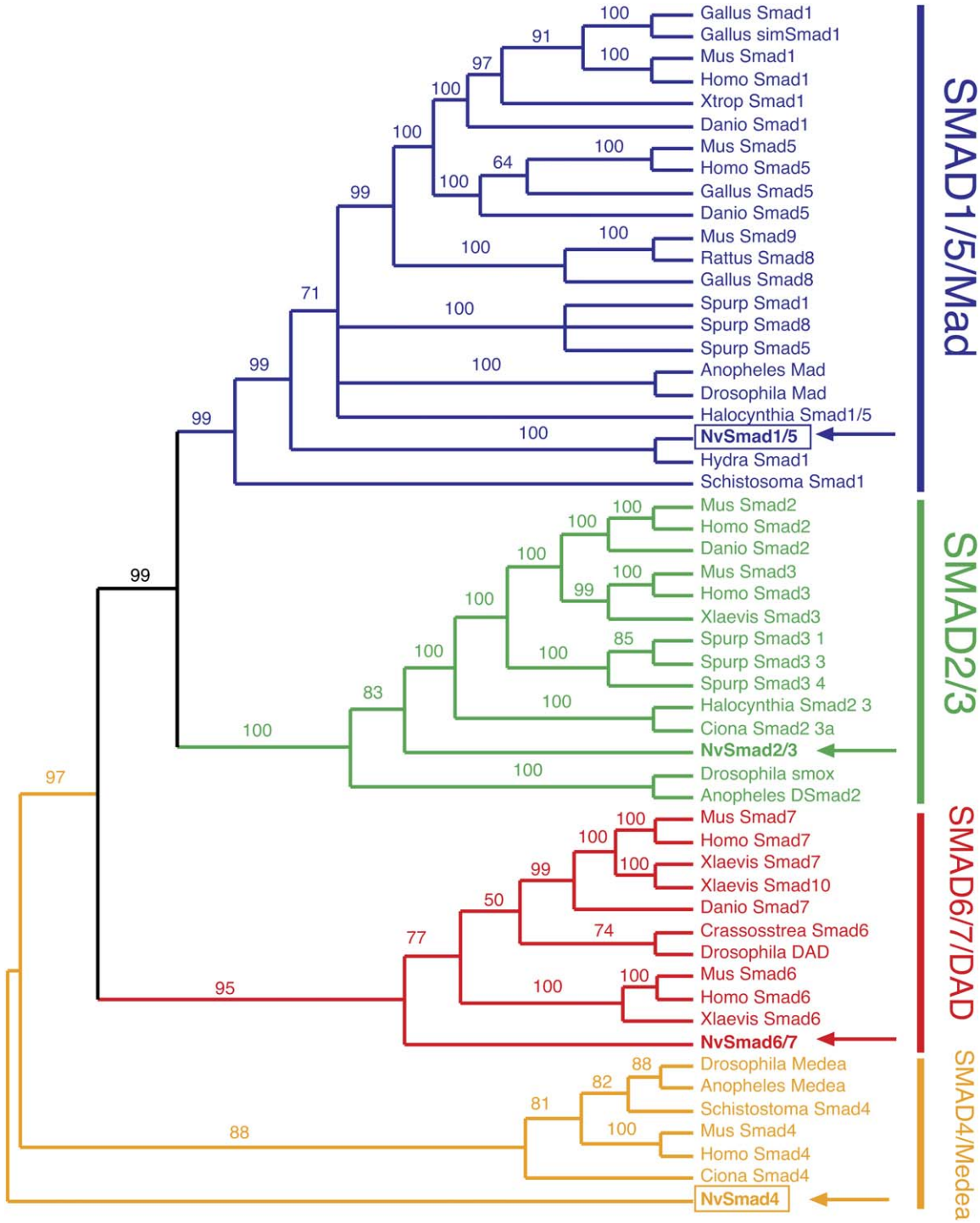

Figure S3. Bayesian Phylogenetic Analysis of Metazoan *Smad* Genes

A Bayesian phylogenetic analysis was conducted with near-full-length amino acid sequences of metazoan Smad orthologs, with the "wag" amino acid model option in MrBayes [S1] and 1,000,000 generations sampled every 100 generations, four chains, and four independent runs. A consensus tree was produced in MrBayes representing 39,500 stationary generations summarizing all four independent runs, with a burnin of 500 trees. Numbers above branches represent posterior probabilities, calculated from this consensus. *N. vectensis* posseses four *Smad* genes, each showing definitive orthology to a specific subclass of Smads. *NvSmad1/5* is an ortholog of vertebrate *Smad1* and *Smad5* genes as well as *Drosophila Mad*. *NvSmad2/3* is an ortholog of vertebrate *Smad2* and *Smad3* genes as well as *Drosophila DSmad2*. *NvSmad6/7* is an ortholog of vertebrate *Smad6* and *Smad7* genes as well as *Drosophila DAD*. *NvSmad4* is an ortholog of vertebrate *Smad4* as well as *Drosophila Medea*.

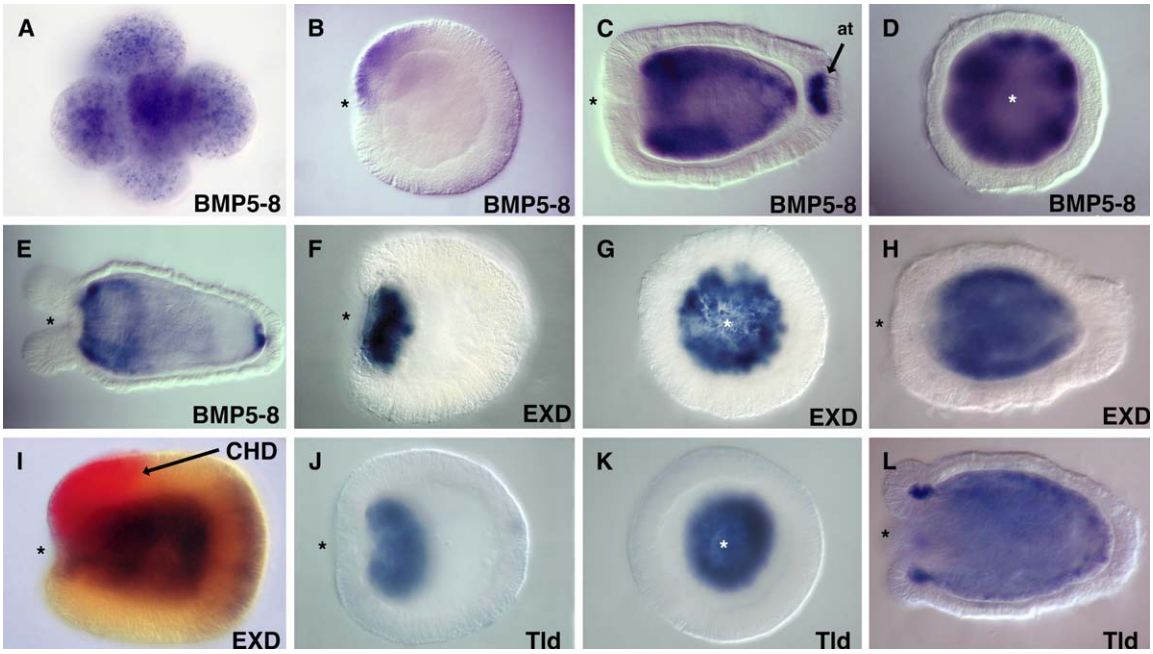

Figure S4. Gene Expression of Bilaterian Dorso/Ventral Patterning Genes in *N. vectensis* Development

(A–E) The TGFβ ligand, *NvBMP5-8*, is expressed maternally (A) and remains expressed throughout cleavage-stage embryos. It is then zygotically expressed asymmetrically on one side of the blastopore during gastrulation (B). (C) In the planula, *NvBMP5-8* is expressed in endoderm as well as in the ectoderm of the apical tuft (at). (D and E) *NvBMP5-8* is expressed in endoderm throughout polyp stages.

(F–H) *NvExd* is expressed at gastrulation in presumptive endoderm at the blastopore and is expressed later in endoderm only (G and H).

(I) Double-label in situ hybridization showing early planula expression of *NvChordin* (red) in oral ectoderm on one side of the directive axis and *NvExd* in endoderm.

(J–L) *NvTolloid* is expressed in invaginating endoderm during gastrulation (J) and later panendodermally including tentacle endoderm (L). The asterisk denotes the blastopore and future mouth. All embryo views are lateral, with anterior to the left, except (A), which is a cleavage-stage embryo, and (D), (G), and (K), which are oral views.

Supplemental References

S1. Huelsenbeck, J.P., and Ronquist, F. (2001). MRBAYES: Bayesian inference of phylogenetic trees. Bioinformatics *17*, 754–755.

S2. Swofford, D.L. (2002). PAUP*: Phylogenetic Analysis Using Parsimony (*and Other Methods) Version 4 (Sunderland, MA: Sinauer Associates).

S3. Technau, U., Rudd, S., Maxwell, P., Gordon, P.M., Saina, M., Grasso, L.C., Hayward, D.C., Sensen, C.W., Saint, R., Holstein, T.W., et al. (2005). Maintenance of ancestral complexity and non-metazoan genes in two basal cnidarians. Trends Genet. *21*, 633–639.

S4. Garcia Abreu, J., Coffinier, C., Larrain, J., Oelgeschlager, M., and De Robertis, E.M. (2002). Chordin-like CR domains and the regulation of evolutionarily conserved extracellular signaling systems. Gene *287*, 39–47.